ELSEVIER

Polymer 42 (2001) 8925–8934

polymer

www.elsevier.com/locate/polymer

Studies on pH and temperature dependence of the dynamics and heterogeneities in poly(*N*-isopropylacrylamide-*co*-sodium acrylate) gels

Tatsuya Motonaga[a], Mitsuhiro Shibayama[b,*]

[a]*Department of Polymer Science and Engineering, Kyoto Institute of Technology, Matsugasaki, Sakyo-ku, Kyoto 606-8585, Japan*
[b]*Neutron Scattering Laboratory, Institute for Solid State Physics, The University of Tokyo, Tokai, Naka-gun, Ibaraki 319-1106, Japan*

Received 16 February 2001; accepted 8 March 2001

Abstract

Dynamic light scattering study has been carried out on weakly charged, temperature-sensitive polymer gels made by copolymerization of *N*-isopropylacrylamide (NIPA) and sodium acrylate (SA) as a function of pH and temperature. The ensemble average light scattering method [Macromolecules 29 (1996) 6535] was employed to extract the thermal component, $\langle I_F \rangle_T$, of the scattered intensity from the ensemble-average scattered intensity $\langle I \rangle_E$ as well as to evaluate the collective diffusion coefficient, D. The following facts were disclosed: (1) The NIPA/SA gels swelled in $4 < pH < 10$, as a result of ionization of acrylic acid (AAc). (2) When pH was varied, $\langle I \rangle_E$ exhibited a maximum around pH 5. This was accounted for by the interplay of the two antagonistic effects on scattered intensity due to ionization of the gel, i.e. (i) an increase in heterogeneities by swelling and (ii) a decrease in heterogeneity due to an increase in osmotic pressure. (3) On the other hand, $\langle I_F \rangle_T$ decreased in the pH region between $5.2 < pH < 10$, due to an increase in osmotic modulus by ionization of the network chains. (4) The variation of D was found to be highly correlated with that of polymer concentration, ϕ, and was scaled to be $D \sim \phi^1$.

Keywords: Dynamic light scattering; Sodium acrylate; *N*-isopropylacrylamide

1. Introduction

Polymer gels undergo swelling or shrinking in response to a change of external stimuli, such as temperature, pH, solvent composition, ionic strength, etc. [1]. These phenomena are analogous to dissolution or precipitation of polymer solutions, respectively. Studies on swelling/shrinking behavior of polymer gels have been accelerated by the discovery of volume phase transition by Tanaka [2]. The volume phase transition is characterized to be a discrete change in volume upon an infinitesimal change of an external stimulus. The transition was observed in a partially ionized polyacrylamide gel in a mixture of water and acetone [2], where the osmotic pressure of counter-ions played an important role in discrete transition. Hirotsu and coworkers investigated volume phase transition for a series of copolymer gels comprising *N*-isopropylacrylamide (NIPA) and sodium acrylate (SA) and reported that the higher the acrylate content (i.e. the higher the ionization), the larger is the volume change on transition [3]. It should be noted, however, that the equilibrium degree of swelling is not governed by counter-ion osmotic pressure, but by Donnan potential emerged in gels [4]. The Donnan potential becomes largest when the difference in the total ionic concentrations between inside and outside of a gel becomes largest [5]. This is why ionized gels swell in moderate pH conditions and shrinks in caustic pH conditions.

Microscopic features of weakly charged gels have been elucidated by small-angle neutron scattering [5,6] and dynamic light scattering (DLS) [7]. It was found that ionized gels have a similar structure to that of a noncharged gel in a good solvent. However, charged gels exhibit a characteristic period of concentration fluctuations due to antagonistic interactions between repulsive (counter-ion and/or Donnan potential) and attractive interactions (hydrophobic and/or van der Waals interaction) when the solvent nature becomes poor [5]. This phenomenon was explained by Khokhlov et al. [8]. When the solvent quality becomes poor, a gel favors a shrunken state to lower the mixing free energy. However, shrinking leads to localization of counter-ions, which has to be attained by a large loss of free energy of the counter-ions. To compromise these two competing contributions to the free energy change, the gel takes another state, a microscopic phase separation to a charged network and noncharged microaggregates, called microaggregates [8]

* Corresponding author. Tel.: +81-29-287-8904; fax: +81-29-287-3922.
E-mail address: sibayama@issp.u-tokyo.ac.jp (M. Shibayama).

0032-3861/01/$ - see front matter
PII: S0032-3861(01)00380-9

or microphase separation [6]. Theories on the basis of this concept was developed by Borue and Erukhimovich [9]. This theory is called a Debye–Hückel theory for polymer solutions. Since the charges are bound on polymer network chains, the characteristic screening length of ionic interaction, i.e. the Debye length, κ^{-1}, is a wave-number dependent. Hence, κ^{-1} is dependent on pH, ionization degree, ionic strength, and dielectric constant of the medium.

Compared to these microscopic aspects, the dynamics as well as spatial heterogeneities of charged polymer gels have been less understood. Though Shibayama et al. [7] studied temperature dependence of collective diffusion coefficient of poly(*N*-isopropylacrylamide/acrylic acid) (NIPA/AAc) gels by DLS, effects of pH on the dynamics and heterogeneities have been unsolved. In this work, we explore pH and temperature dependence of the dynamics and spatial heterogeneities of weakly charged polymer gels made of NIPA and SA and discuss the role of charges and counterions on the volume phase transition as well as the dynamics of collective diffusion.

2. Experimental section

2.1. Samples

NIPA monomer, supplied by Kohjin, Co. Ltd, Tokyo, was purified by dissolving in toluene and recrystallizing in petroleum ether. 658 mM of NIPA monomer, 32 mM of SA, 8.62 mM of *N*,*N*′-methylenebisacrylamide (BIS; cross-linker), and 1.75 mM of ammonium persulfate (APS; initiator) were dissolved in distilled water and degassed. After chilling the solution in a refrigerator, 8 mM of *N*,*N*,*N*′,*N*′-tetramethylethylene diamine (TEMED; accelerator) was added in order to initiate redox copolymerization as well as cross-linking. The polymerization was conducted at 20°C for 24 h. In the case of samples for swelling experiments, gels were made in a 10 μl-micropipette (the inner diameter being 471 μm). Samples for DLS measurements were made in a test tube with inner diameter of 4 mm, which was small enough for spontaneous swelling in a larger test tube at a given pH. The gels thus prepared were taken out from the mold and washed in distilled water, then transferred to a laboratory-made chamber with glass windows (for swelling measurement under a microscope) and to another test tube with 8 mm diameter (for DLS).

2.2. DLS

DLS studies were carried out on a static/dynamic compact goniometer (SLS/DLS-5000), ALV, Langen, Germany. A He–Ne laser with 22 mW was used as the incident beam. The temperature of the sample was regulated with a Neslab 110 RT, Neslab Instruments, Co., Portsmouth, NH. The step of the temperature change was set less than 5 or 0.5°C, depending on the temperature range far from or close to the transition temperature, and more than 10 days was paused before DLS measurements not only for thermal equilibration, but also for swelling equilibration of the gel.

3. Results and discussion

3.1. Swelling curves

Fig. 1 shows the swelling curve of NIPA/SA gel as a function of pH. The observation temperature was 20°C. d and d_0 denote, respectively, the gel diameter at observation and that at preparation, i.e. the mold diameter. The linear swelling ratio, d/d_0, increased rapidly with pH in the region of $4 \leq \text{pH} \leq 6$, which is due to ionization of AAc. A highly swollen state lasted until pH $\approx$ 10 and then d/d_0 decreased as a result of an increase in the screening effect of electrostatic interactions as discussed elsewhere [5].

Fig. 2 shows variations of d/d_0 with temperature for gels conditioned at various pH values. For comparison, that of NIPA homopolymer, which does not ionize in any pH, is also given at the top-left corner. Here, results of two types of swelling experiments are shown. One was done in a closed cell and the other in an open cell. In the case of the closed cell, the cell was isolated from reservoir after adjusting pH. On the other hand, the open cell means that a swelling measurement was carried out by keeping a flow of pH-adjusted water. As discussed in Fig. 1, d/d_0 at $T = 20$°C increases with pH up to 9, and then decreases with further increasing pHs. Regarding temperature dependence, d/d_0 gradually decreases with temperature at all pHs. However, it is noted that there exists a discrete volume change in the homopolymer and copolymer gels exclusively at low pHs, e.g. 3.0, 5.58, and 5.71. This phenomenon, i.e. the volume phase transition, is well known as volume phase transition of polymer gels and is interpreted with thermodynamic theories by Tanaka et al. [2,10]. Interestingly, however,

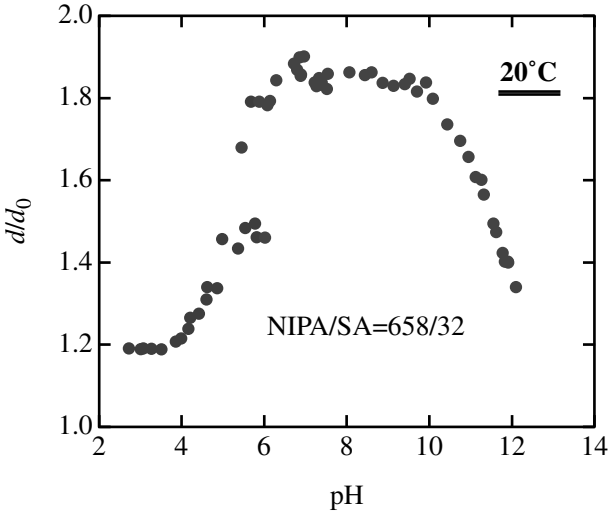

Fig. 1. pH dependence of the degree of swelling, d/d_0, for NIPA/SA gel measured at 20°C.

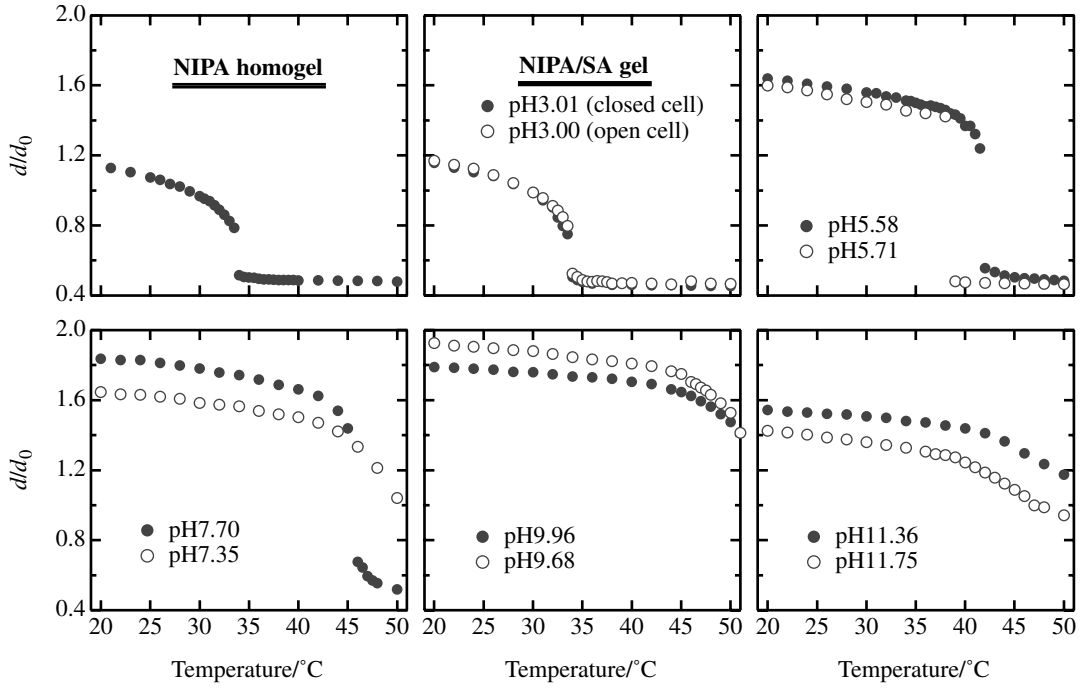

Fig. 2. Temperature dependence of d/d_0 for NIPA homopolymer (the top-left) and NIPA/SA gels conditioned at various pHs (others). Open and filled symbols denote the values of d/d_0 for gels in an open cell and in a closed cell, respectively.

there appeared two significant features in the swelling behavior whether or not the cell is closed: (1) At pH 5.58 and 5.71 region, the transition temperature for the case of closed cell is higher by ca. 3° than that of the open cell. (2) At pH 7.70 and 7.35, the gel in the open cell undergoes a continuous transition, while that in the closed cell still exhibits a discrete transition. The original Tanaka's theory [2] cannot predict such a phenomenon since it simply introduces an osmotic free energy of counter-ions. Several modified theories have been proposed to explain swelling behavior of ionized gels by incorporating Donnan potential [4,5,11]. However, an additional concept, i.e. temperature dependence of the ionization constant is also required to explain the phenomenon disclosed above.

Fig. 3 shows the ionization curves for poly(acrylic acid) aqueous solutions as a function of pH for 25, 35, and 40°C. The values of pK_a were evaluated from the data reported by Kawasaki et al. [12] where K_a is the ionization constant. These curves were obtained by using Henderson–Hasselbach equation given by [13,14]

$$pK_a = pH - \log[\alpha/(1-\alpha)] \quad (1)$$

where α is the degree of ionization. This indicates that the ionization curve shifts to the higher pH region by increasing temperature. This results in a decrease in the ionization for the case of open cell as shown by the solid arrow, giving rise to a shift of the transition temperature to a higher temperature. On the other hand, in the case of closed cell, ions are not provided to the gel from the reservoir even if the pK_a is changed by temperature. As a result, the pH of the gel is expected to increase as shown by the dashed arrow. The lowering of ionization keeps the occurrence of a discrete volume transition. The change of a discrete to continuous transitions is discussed by Kawasaki et al. [12] and Sasaki et al. by taking account of the change of the solvent activity [15].

The question is why the gel in a closed gel at pH 7.70 is discrete and that in an open cell at pH 7.35 is continuous. The osmotic pressure due to Donnan membrane effect, Π_{Donnan}, is determined by the difference in the ion concentrations inside and outside a gel, i.e. [4]

$$\Pi_{\text{Donnan}} = -\frac{\Delta\mu_{\text{ion}}}{V_s} \approx RT\,\Delta C \quad (2)$$

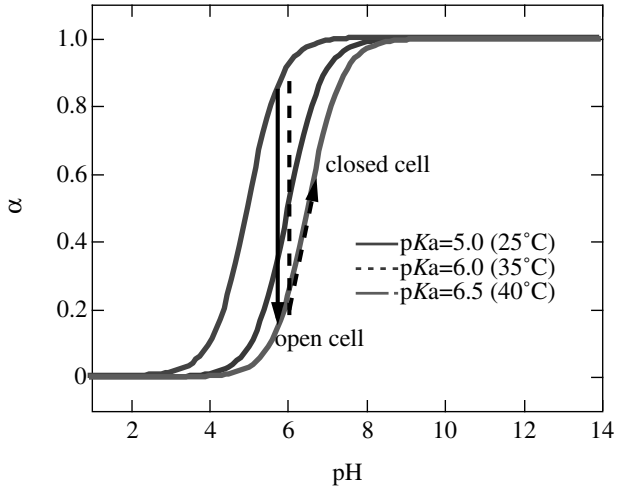

Fig. 3. pH dependence of the degree of ionization, α, for polyacrylate aqueous solutions.

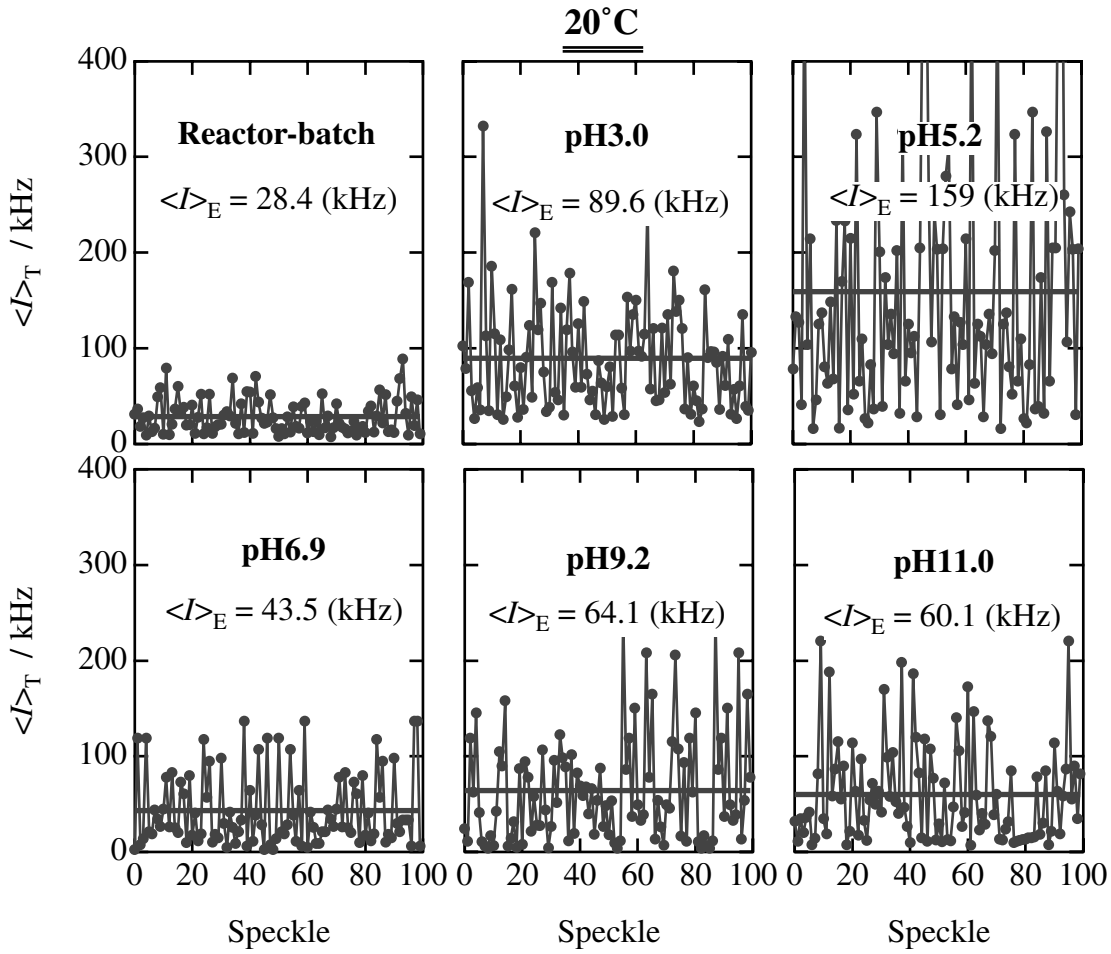

Fig. 4. Speckle patterns of NIPA/SA gels in a reactor batch and conditioned at various pHs. The horizontal solid lines indicate the ensemble average scattered intensity, $\langle I \rangle_E$.

where V_s is the molar volume of the solvent, $\Delta\mu_{ion}$ is the contribution of mobile ions to the chemical potential, R is the gas constant, and ΔC is the difference in mobile ion concentrations inside and outside the gel. Let us consider a case, a pH region near the isoelectric point. If the sample cell is isolated, the provided ions are fed by acrylate ions to neutralize. On the other hand, if a gel is in an open cell, ions are provided by the reservoir. Therefore, the following inequality is given: $\Delta C_{open} < \Delta C_{closed}$. This leads to a discrete transition for a gel in a closed cell and a continuous transition for a gel in an open cell at the pH region of 7–8. For higher pHs, which is attained by adding more NaOH to the reservoir, ΔC becomes even less, resulting in a lowering of d/d_0.

3.2. DLS

3.2.1. pH dependence

Fig. 4 shows time-average scattered intensity obtained at different sample positions, $\langle I \rangle_T$, conditioned at different pHs. As shown in the figure, $\langle I \rangle_T$ scatters vigorously with sample position. This is one of the characteristic features of gels due to nonergodicity, called speckle pattern [16–18]. Due to the presence of cross-links, translational diffusion of polymer chains is prohibited, which leads to nonzero-sum cancellation of the concentration fluctuations in the system, resulting in a strong increase in the scattered intensity. The ensemble average scattered intensity, $\langle I \rangle_E$ (shown by the horizontal solid line), was obtained by taking the average of $\langle I \rangle_T$ over 100 points for each sample. $\langle I \rangle_E$ increases by swelling, i.e. from the reactor-batch gel to pHs 3.0 and 5.2, and then decrease by further increase in pH.

Fig. 5 shows the variation of $\langle I \rangle_E$ with pH. The dashed line indicates $\langle I \rangle_E$ for a gel in a reactor batch (at pH $\approx$ 10), which is shown for comparison. First of all, it is clear that $\langle I \rangle_E$ increases by immersing the gel in a pH-conditioned solution. The increase in $\langle I \rangle_E$ with pH around 5 may be explained by the following two facts. One is ascribed to swelling of the gel by ionization (see Fig. 1). It is known that at least for noncharged neutral gels, the higher the swelling, the larger are the heterogeneities (i.e. the larger in $\langle I \rangle_E$) [19]. This is due to the fact that spatial heterogeneities in

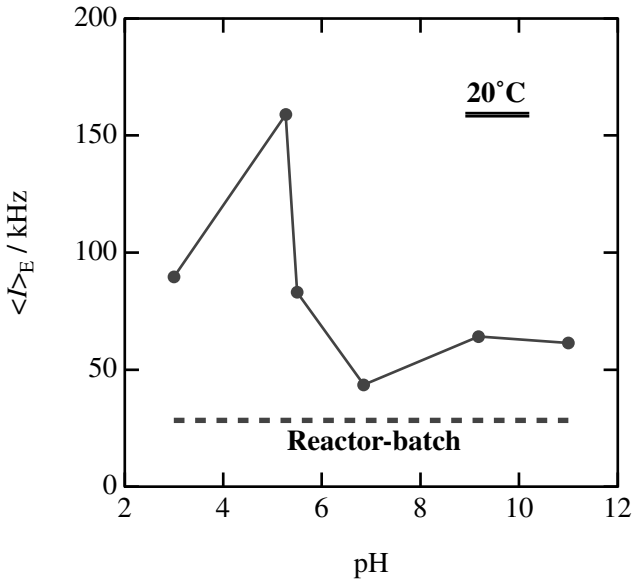

Fig. 5. Variation of $\langle I\rangle_E$ with pH for NIPA/SA gel at 20°C. The dashed line indicates $\langle I\rangle_E$ for reactor-batch gel.

cross-linking point variation becomes explicit by swelling as discussed by Bastide and Leibler [20] and Mendes et al. [21]. The following stepwise decrease in $\langle I\rangle_E$ for pH > 6 is puzzling. The other is an increase in the osmotic pressure in the gel, which strongly suppresses the concentration fluctuations, i.e. a decrease in $\langle I\rangle_E$. As a matter of fact, scattered intensity from a charged gel, in general, is much lower than a noncharged gel. This is why the maximum of $\langle I\rangle_E$ is located around the infection point in the pK_a vs pH curve (Fig. 3).

Fig. 6 shows the time–intensity correlation functions (ICF), $g^{(2)}(\tau)$, for NIPA/SA gel at pHs 3.0 5.2, 6.9, 9.2, and 11.0 measured at 20°C. The sample position was arbitrarily chosen. Hence, it should be noted that the ICF itself was sample position dependent. The ICF is defined by

$$g^{(2)}(\tau) \equiv g^{(2)}(\tau;\mathbf{q}) = \frac{\langle I(0;\mathbf{q})I(\tau;\mathbf{q})\rangle_T}{\langle I(0;\mathbf{q})\rangle_T^2} \tag{3}$$

where, $I(\tau;\mathbf{q})$ is the scattered intensity at time lag τ with respect to $\tau = 0$ and at the scattering vector $\mathbf{q}$, and $\langle\cdots\rangle_T$ denotes time average. In the case of gels, $g^{(2)}(\tau)$ is often represented by a single exponential function as given by [22]

$$g^{(2)}(\tau) - 1 = \sigma_I^2 \exp(-2D_A\mathbf{q}^2\tau) \tag{4}$$

where σ_I^2 is the initial amplitude of ICF and D_A is the apparent diffusion coefficient. As shown in these figures, all the observed ICFs are well fitted with Eq. (4) within errors of 10^{-3} as indicated with dots and the right axis. Note that the initial amplitude is much less than unity for most of the gels as a result of nonergodic nature [16].

The apparent diffusion coefficient, D_A, was more rigorously evaluated by taking the slopes of $\ln[g^{(2)}(\tau) - 1]$ vs τ plot, i.e.

$$D_A = -\frac{1}{2\mathbf{q}^2}\frac{\partial}{\partial\tau}\ln[g^{(2)}(\tau) - 1]_{\tau=0} \tag{5}$$

for all sample positions in each sample. By plotting $\langle I\rangle_T/D_A$ as a function of $\langle I\rangle_T$, one obtains the collective diffusion coefficient D and the dynamic component of the scattered intensity, $\langle I_F\rangle_T$, owing to the following relationship [7]:

$$\frac{\langle I\rangle_T}{D_A} = \frac{2}{D}\langle I\rangle_T - \frac{\langle I_F\rangle_T}{D} \tag{6}$$

Fig. 7 shows the case of pH 3.0 at 20°C, from which D and $\langle I\rangle_T$ were obtained to be 4.84×10^{-7} cm^2/s and $\langle I_F\rangle_T = 18.8$ kHz. The same analysis was applied to all the gels at various pHs and temperatures.

Fig. 8a shows the pH dependence of D for the gel at 20°C. It is interesting to note that the variation of D with pH is quite similar to that of d/d_0 (see Fig. 1). It is known that the correlation length, ξ, for semidilute polymer solutions in a good solvent scales with $\phi^{-3/4}$ [23], where ϕ is the polymer volume fraction in the gel. Since the collective diffusion coefficient D is inversely proportional to ξ, one expects

$$D \sim \phi^{3/4} \sim (d/d_0)^{-9/4} \tag{7}$$

In Fig. 8b and c are plotted $D\phi^{-3/4}$ vs pH, and $D\phi^{-1}$ vs pH. The results indicate that D scales with ϕ^1 rather than $\phi^{3/4}$. Though the origin of the contradiction between the theoretical prediction ($D \sim \phi^{3/4}$) and the experimental result ($D \sim \phi$) is not clear at this stage, it is clear that the variation of D is strongly correlated with that of d/d_0. This means that the collective diffusion coefficient is mainly governed by the polymer concentration in a gel.

Fig. 9 shows the pH dependence of $\langle I_F\rangle_T$, $\langle I\rangle_E$, and the ratio of $\langle I\rangle_E/\langle I_F\rangle_T$. Note that $\langle I\rangle_E/\langle I_F\rangle_T$ is a measure of the degree of heterogeneity, and $\langle I_F\rangle_T$ and $\langle I\rangle_E$ are plotted in the logarithmic scale to compare the magnitude of variations with pH. By comparing the variation of $\langle I\rangle_E$ with pH, that of $\langle I_F\rangle_T$ is much larger, indicating that the dynamic fluctuations are more strongly dependent on pH (or ionization). On the other hand, the variation of the degree of heterogeneity with pH is very similar to that of d/d_0. This indicates that the degree of heterogeneity is strongly correlated with the degree of swelling, as is the case of noncharged gels of which origin is discussed by Bastide and Leibler [20].

3.2.2. Temperature dependence

In the case of NIPA gels, the scattered intensity increases with increasing temperatures and diverges at the volume transition temperature $\approx$ 34°C [7,24]. This is due to hydrophobic nature of NIPA chains. A series of plots of $\langle I\rangle_T$ at various sample positions for NIPA/SA gels observed at pH 3.0 are shown in Fig. 10, which reproduce such temperature dependence of $\langle I\rangle_T$ for NIPA gels although about 4.6 mol% of NIPA was replaced by SA. This is reasonable since the acrylate group does not ionize at pH 3.0, and the swelling

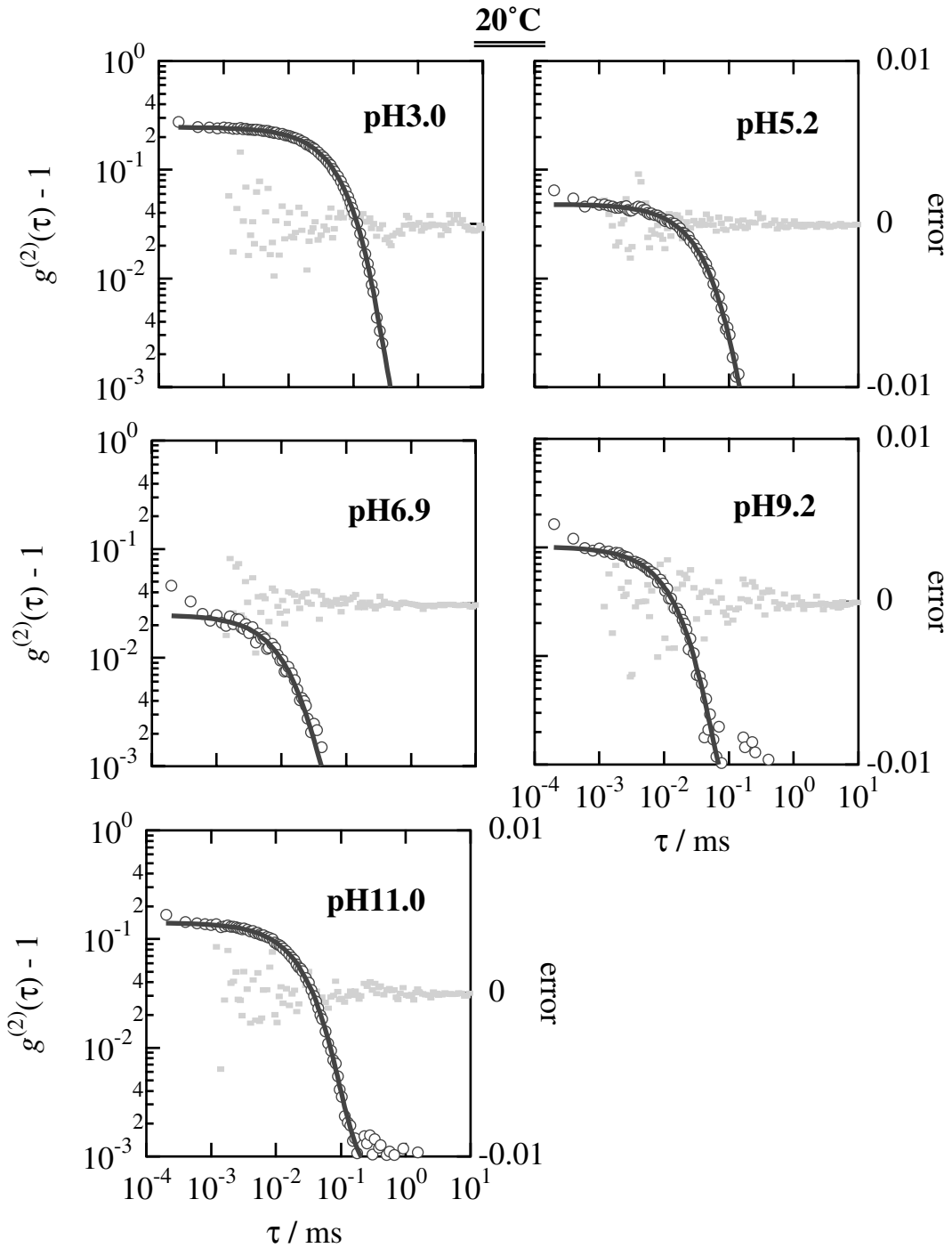

Fig. 6. Series of time–intensity correlation functions, ICF, for NIPA/SA gels conditioned at various pHs. The solid lines denote the fit with a single exponential function and the dots represent the error of the fit.

behavior is similar to that of NIPA homopolymer gels (see Fig. 2). Both $\langle I \rangle_E$, denoted by the horizontal solid line, and the magnitude of the intensity fluctuations in speckles increased with temperature.

Fig. 11 shows temperature dependence of $\langle I \rangle_E$ for the gels at different pH values. The gel at pH 3.0 shows a steep upturn in $\langle I \rangle_E$, indicating a divergence in $\langle I \rangle_E$ as a result of volume phase transition. A similar upturn is also expected for the gels at pH 5.2. A symptom of upturn was observed at 37.5°C for the case of pH 5.2, but a further increase in temperature may be required to observe a divergence in $\langle I \rangle_E$. On the other hand, such divergence may not take place at pH 11.0 because a continuous transition in d/d_0 is observed (see Fig. 2).

Fig. 12 shows ICFs for pH 3.0 at 33.5°C fitted by (a) single exponential function and by (b) a stretched exponential

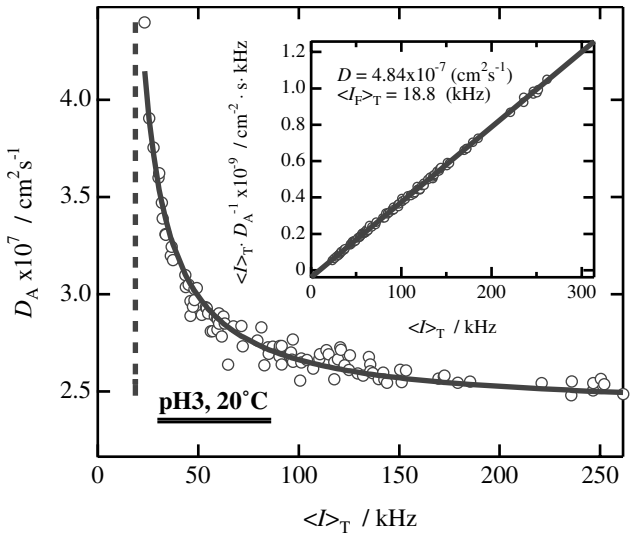

Fig. 7. Plot of the apparent diffusion coefficient, D_A, vs time-average scattered intensity, $\langle I\rangle_T$. The vertical dashed line indicate the lower bound of $\langle I\rangle_T$ ($\equiv \langle I_F\rangle_T$). The inset indicates the linearized plot to evaluate the collective diffusion coefficient, D, and the fluctuating component in the scattered intensity $\langle I_F\rangle_T$.

function. It is clear that the observed ICF cannot be fitted with a single exponential function. The stretched-exponential-function fit employs the following function, a combination of a single exponential and a stretched-exponential functions, i.e.

$$g^{(2)}(\tau) - 1 = \sigma_I^2\{A\exp(-D_A\mathbf{q}^2\tau) + (1-A)\exp[-(\tau/\tau_{slow})^{\beta}]\}^2 \quad (8)$$

where A is the fraction of the fast mode, i.e. the collective diffusion mode, τ_{slow}, is the characteristic decay time for the slow mode, and β is the stretched exponent. The estimated values by fitting were $A = 0.53$, $\tau_{slow} = 731$ ms, and $\beta = 0.59$. This suggests that the dynamics of gels near the transition point cannot be described by a collective diffusion mode, but a slower diffusion mode has also to be taken into account as a result of emergence of a long-range concentration fluctuations. In the previous paper, we employed a double exponential function fit to ICFs for similar gels [7]. However, since the decay-time window was very limited to be 2×10^{-2} to 10 ms, an erroneous conclusion was drawn. The observed ICF with a much wider time range as well as a fit with Eq. (8) shown in Fig. 12b suggests that a stretched-exponential-function fit is preferable and a slow mode with $\tau_{slow} \approx 731$ ms is present. The appearance of the slow mode may indicate a formation of microaggregated domains due to the interplay of strong hydrophobicity and electroneutrality as discussed by Khokhlov [8].

Fig. 13 shows the temperature dependence of D for gels at pHs 3.0, 5.2, and 11.0. A critical slowing down [23] is observed for pHs 3.0 and 5.2 by approaching the transition temperature. It is noteworthy that on the other hand, D for pH 11.0 exhibits the opposite temperature dependence. This

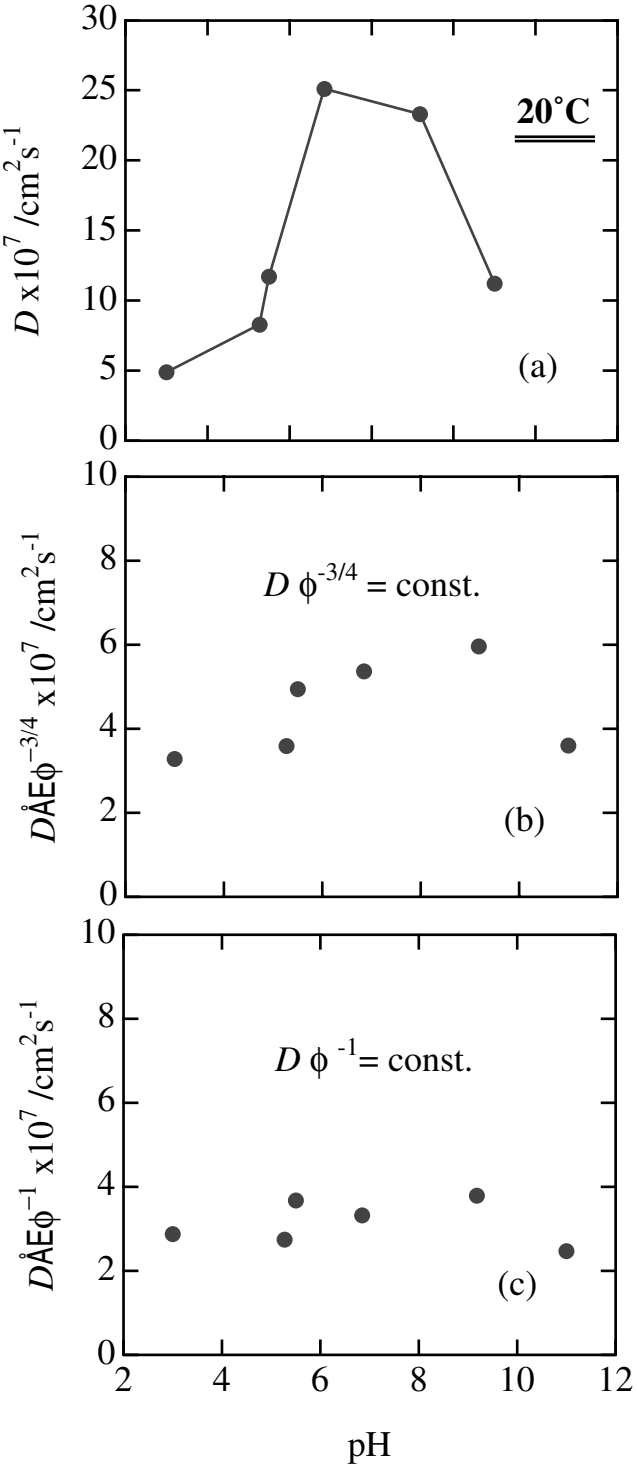

Fig. 8. pH dependence of (a) D, (b) $D\phi^{-3/4}$, (c) $D\phi^{-1}$ for NIPA/SA gel at 20°C.

behavior can be explained as follows: the collective diffusion coefficient D is related to the correlation length ξ, via

$$D = \frac{kT}{6\pi\eta\xi} \quad (9)$$

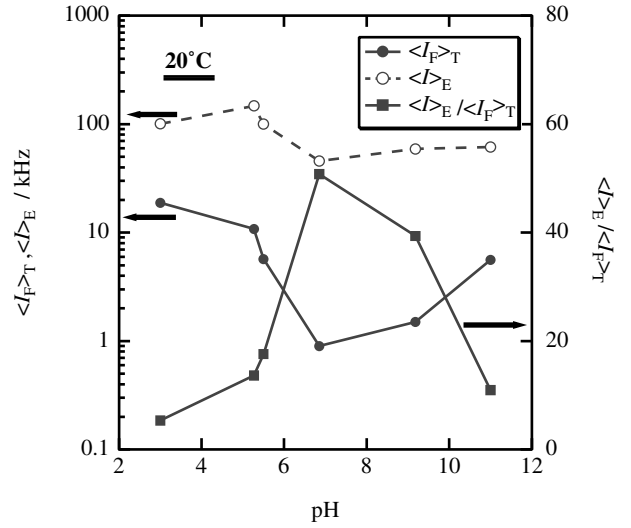

Fig. 9. pH dependence of $\langle I\rangle_E$, $\langle I_F\rangle_T$ and the degree of heterogeneity, $\langle I\rangle_E/\langle I_F\rangle_T$ for NIPA/SA gel at 20°C.

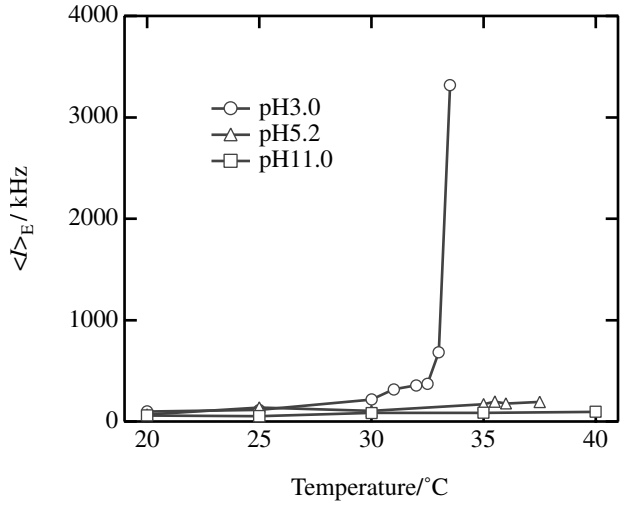

Fig. 11. Temperature dependence of $\langle I\rangle_E$ for NIPA/SA gels conditioned at pHs 3.0, 5.2, and 11.0.

where η is the viscosity of the medium, k, the Boltzmann constant, and T, the absolute temperature. In the case of pHs 3.0 and 5.2, the variation of ξ with T is much larger than that of η, resulting in an observation of critical slowing down, i.e. a decrease in D with T was observed. However, for pH 11, ξ may be rather invariant since the temperature is still far away from the transition temperature. On the other hand, the viscosity of the medium, i.e. water, decreases roughly by a factor of two in this temperature range (1.01 cPa at 20°C to 0.62 cPa at 40°C). This is why D decreases with T.

Fig. 14 shows the variation of ξ with temperature for gels at pHs 3.0, 5.2, and 11.0. As shown in the figure, ξ seems to diverge by approaching the transition temperature. The inset shows the log–log plot of ξ vs $|T - T_c|/T_c$. The critical exponent was evaluated to be 0.56, which is in between the mean-field and Ising prediction [25,26]. In the previous article, we reported that the critical exponent was 0.63 on the basis of small-angle neutron scattering [27]. The disagreement of the exponent may be explained as follows. Gels can be regarded as an assembly of uncorrelated domains in which spatial correlation holds and the size of each domain is of the order of wavelength of light or less. This is why a speckle is observed in a gel due to nonvanishing interference of scattered light and nonergodicity is **q**-dependent [16]. Since the wave-number used in light scattering ($\sim$0.001 Å^{-1}) is about 100 times smaller than that of small-angle neutron scattering ($\sim$0.1 Å^{-1}), critical phenomena were observed more mean-field like due to the coverage of a wider range of uncorrelated domains by light scattering. It is needless to mention that a further investigation is required to answer this question.

4. Conclusions

The swelling behavior and the chain dynamics of weakly charged polymer gels consisting of poly(*N*-isopropylacrylamide-*co*-sodium acrylate) gels were investigated by

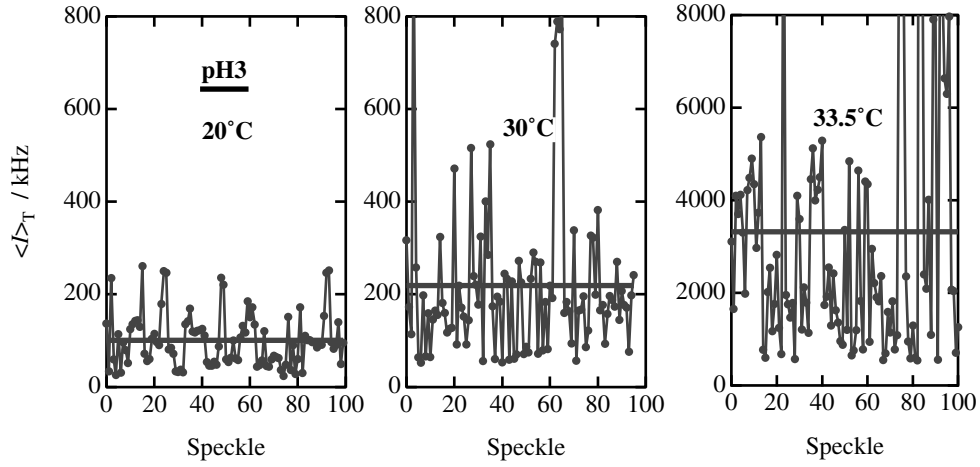

Fig. 10. Speckle patterns of NIPA/SA gel (pH 3.0) at 20, 30, and 33.5°C. The horizontal line indicates $\langle I\rangle_E$.

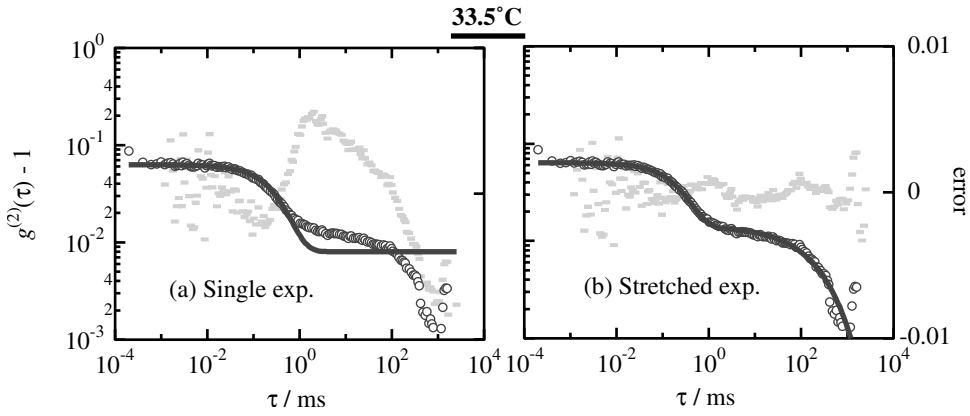

Fig. 12. ICFs for NIPA/SA gel at 33.5°C and pH 3.0 and fits with (a) single-exponential and (b) stretched-exponential functions. The solid lines are the fits with Eqs. (4) and (8), respectively.

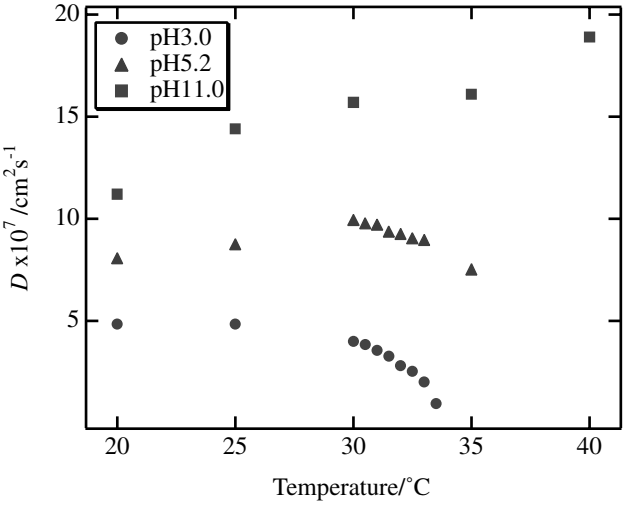

Fig. 13. Variation of D with temperatures for NIPA/SA gels conditioned at pHs 3.0, 5.2, and 11.0.

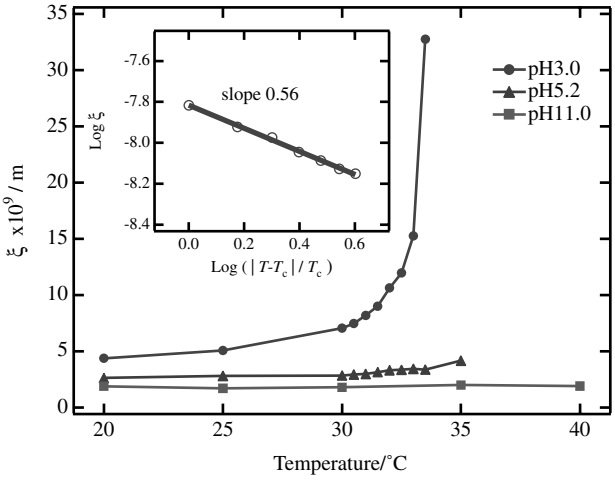

Fig. 14. Temperature dependence of the correlation length, ξ, for NIPA/SA gels conditioned at pHs 3.0, 5.2, and 11.0. The inset shows the double logarithmic plot of ξ and the reduced temperature, $|T - T_c|/T_c$.

swelling and DLS experiments as a function of pH and temperature. The following facts were disclosed: (1) The degree of swelling increased with pH in the medium pH regions, i.e. $4 < \mathrm{pH} < 10$. This is due to ionization of acrylate groups. However, the swelling degree decreases by further increase in pH as a result of electric screening effect. (2) When pH was varied, $\langle I \rangle_E$ exhibited a maximum around pH 5. This was accounted for by the interplay of the two antagonistic effects on scattered intensity due to ionization of the gel, i.e. (i) an increase in heterogeneities by swelling and (ii) a decrease in heterogeneity due to an increase in osmotic pressure. (3) The ensemble-average DLS experiments allowed us to evaluate the collective diffusion coefficient, D, and the degree of heterogeneity, $\langle I \rangle_E / \langle I_F \rangle_T$. (4) It was obtained that the variation of $\langle I \rangle_E / \langle I_F \rangle_T$ with pH is very similar to that of the swelling curve. Hence, it is concluded that the degree of heterogeneity is mainly governed by the polymer concentration for gels with a fixed cross-link concentration. (5) The collective diffusion coefficient D varied with $D \sim \phi^{-1}$ and exhibited a critical slowing down by approaching the transition temperature, of which critical exponent for correlation length was estimated to be 0.56.

Acknowledgements

This work is partially supported by the Ministry of Education, Science, Sports and Culture, Japan (Grant-in-Aid, 12450388).

References

[1] Tanaka T. Sci Am 1981;244:110.
[2] Tanaka T. Phys Rev Lett 1978;40:820.
[3] Hirotsu S, Hirokawa Y, Tanaka T. J Chem Phys 1987;87:1392.
[4] Moe ST, Skjak-Break G, Elgsaeter A, Smidsrod O. Macromolecules 1993;26:3589.
[5] Shibayama M, Ikkai F, Inamoto S, Nomura S, Han CC. J Chem Phys 1996;105:4358.
[6] Shibayama M, Tanaka T, Han CC. J Chem Phys 1992;97:6842.

[7] Shibayama M, Fujikawa Y, Nomura S. Macromolecules 1996;29:6535.
[8] Khokhlov AR, Philippova OE, Sitnikova NL, Starodoubtsev SG. Faraday Discuss 1995;101:125.
[9] Borue V, Erukhimovich I. Macromolecules 1988;21:3240.
[10] Shibayama M, Tanaka T. Adv Polym Sci 1993;109:1.
[11] Khokhlov A, Starodoubtsev SG, Vasilevskaya VV. Adv Polym Sci 1993;109:123.
[12] Kawasaki H, Sasaki S, Maeda H. J Phys Chem B 1997;101:5089.
[13] Katchasky A, Spitnik P. J Polym Sci 1947;2:432.
[14] Seno M, Lin ML, Iwamoto K. Colloid Polym Sci 1991;269:873.
[15] Sasaki S, Maeda H. J Chem Phys 1997;107:1028.
[16] Pusey PN, van Megen W. Physica A 1989;157:705.
[17] Joosten JGH, McCarthy JL, Pusey PN. Macromolecules 1991;24:6690.
[18] Shibayama M. Macromol Chem Phys 1998;199:1.
[19] Shibayama M, Shirotani Y, Shiwa Y. J Chem Phys 2000;112:442.
[20] Bastide J, Leibler L. Macromolecules 1988;21:2647.
[21] Mendes EJ, Lindner P, Buzier M, Boue F, Bastide J. Phys Rev Lett 1991;66:1595.
[22] Tanaka T, Hocker LO, Benedek GB. J Chem Phys 1973;59:5151.
[23] de Gennes PG. Scaling concepts in polymer physics. Ithaca: Cornell University, 1979.
[24] Shibayama M, Tanaka T, Han CC. J Phys (Paris) IV 1993;C8:25.
[25] Stanley HE. Introduction to phase transition and critical phenomena. New York: Oxford University Press, 1971.
[26] Li Y, Tanaka T. J Chem Phys 1989;90:5161.
[27] Shibayama M, Tanaka T, Han CC. J Chem Phys 1992;97:6829.